

EXPLOITING BURSTING DYNAMICS FOR ENHANCED ENERGY HARVESTING AND VIBRATION CONTROL

Michele Rosso¹ and Raffaele Ardito¹
¹Politecnico di Milano, ITALY

ABSTRACT

In this work, we investigate bursting dynamics in piezoelectric energy harvesters as a strategy to enhance performance under low-frequency (<10 Hz) excitations. A mesoscale bistable harvester with permanent magnets is modeled and numerically simulated, showing that bursting regimes enable efficient frequency up-conversion, providing an alternative to approaches based on moving proofmasses. Compared to classical inter-well oscillations, bursting yields a substantial increase in harvested power, with representative steady-state values of about 3.5 mW on a 50 kΩ load. These results highlight the potential of bursting dynamics not only for energy harvesting from sources such as human motion, but also for vibration control and programmable devices.

KEYWORDS

Bursting vibrations, piezoelectric energy harvesting, nonlinear dynamics.

INTRODUCTION

Over the past 15 years, the field of energy harvesting has focused on introducing various forms of nonlinearity to enhance system performance, through both mechanical [1] and electronic [2] strategies. This interest is motivated by the need to overcome the inherent limitations of linear resonant devices, which typically exhibit narrow bandwidths and limited efficiency under broadband or low-frequency excitations, such as those generated by ambient vibrations [3]. Among the different nonlinear approaches, magnetic interaction-based harvesters have attracted considerable attention due to their ability to achieve broadband responses and frequency up-conversion, which are highly desirable features for real-world applications [4].

Many studies have focused on designing new devices, either to achieve miniaturization or to improve performance through careful material choice and optimization of external excitation forces. More recently, however, attention has shifted toward peculiar nonlinear dynamic regimes that may emerge in such systems. One particularly intriguing phenomenon is represented by bursting dynamics, which arise when intra-well oscillations are superimposed on inter-well vibrations [5]. While this behavior has been extensively studied in applied mathematics [6] and biology [7], its potential for energy harvesting remains largely unexplored. Importantly, it is not yet clear whether the parameter ranges that support bursting dynamics can be realistically achieved in meso- and MEMS-scale devices.

In this work, we numerically show the effect of bursting dynamics using a classical bistable piezoelectric energy harvester. By tuning the design parameters without altering the magnetic configuration, the system's performance can be significantly enhanced. This result

suggests that existing, well-studied devices can be adaptively optimized to improve dynamic response, without the need for redesigning the structure. Beyond energy harvesting, the proposed approach opens perspectives in vibration control, where energy transfer across different frequencies could be deliberately modulated by suitable tuning.

The paper is structured as follows. First, the layout of the system and the modeling strategy are presented. Then, the numerical investigation is presented and discussed. Finally, concluding remarks are provided in the last section.

CONCEPTUAL DESIGN AND MODELING

The system considered in this study is illustrated in Fig. 1.

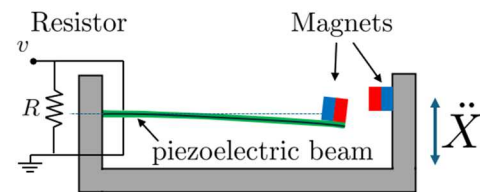


Figure 1: schematic of the energy harvesting device.

The system illustrated in Fig. 1 exhibits a bistable potential due to the repulsive configuration of the magnets. A piezoelectric bimorph cantilever is clamped on a frame that oscillates harmonically under the action of an external acceleration \ddot{X} . The mathematical model of the system was developed using a lumped-parameter approach, with one degree of freedom for each physical domain. Specifically, x denotes the mechanical degree of freedom associated with the cantilever tip displacement, while v represents the voltage across the free electrode. This modeling choice allows to retain the essential electromechanical coupling and nonlinear magnetic interaction while keeping the computational burden low, which is particularly advantageous for extensive parametric studies. Although distributed or finite element formulations could capture additional details, previous works have shown that lumped-parameter models provide accurate predictions of the dynamic behavior. The harvester is connected to a purely resistive circuit. Analytical details of the modeling approach can be found in [8]. The nonlinear contribution arises exclusively from the magnetic interaction. The governing equations of motion are:

$$\begin{cases} m\ddot{x} + c\dot{x} + kx - \vartheta v = f_{ext} + f_{mag} \\ C\dot{v} + \vartheta\dot{x} + \frac{v}{R} = 0 \end{cases} \quad (1)$$

where m is the total effective mass, c is the linear damping

coefficient, derived from the quality factor Q , and k is the linear stiffness of the cantilever. The parameter ϑ is the electromechanical coupling constant, while C is the equivalent capacitance of the piezoelectric layers. The dielectric constant of vacuum is assumed to be $\epsilon_0=8.854\times 10^{-12}$ F/m. The external force f_{ext} corresponds to the imposed harmonic acceleration, whereas f_{mag} represents the nonlinear magnetic interaction force produced by the permanent magnets. The magnets used in this work are cubic (side length 3 mm) with a magnetization of 1.32 T, as reported in [8]. The geometrical and physical parameters adopted in the numerical simulations are summarized in Table 1.

Table 1: Geometrical and physical parameters of the system

Parameter	Value	Description
b	18 mm	Cantilever width
L	67 and 68 mm	Cantilever length
L_p	60 mm	PZT layer length
t_{tit}	210 μ m	Titanium thickness
t_{PZT}	180 μ m	PZT thickness
E_{tit}	115 GPa	Titanium Young's Modulus
E_{PZT}	60 GPa	PZT Young's Modulus
e_{31}	-12 N/(mV)	31 piezoelectric constant
$\epsilon_{33}^s(\epsilon_0)$	2000	Relative dielectric constant
ρ_{tit}	4.5 g/cm ³	Titanium unit mass
ρ_{PZT}	7.5 g/cm ³	PZT unit mass
h	2 mm	Gap between magnets
Q	200	Quality factor
R	50 k Ω	Load resistor

NUMERICAL RESULTS AND DISCUSSION

The system described by Eq. (1) was implemented in MATLAB and solved using the Runge–Kutta method. Time-domain simulations were performed over an interval of 5 s, sufficiently long considering the natural frequency of the corresponding linear system, about 73.12 Hz (with a titanium substrate length of 61 mm). Three cases were compared: (i) purely harmonic excitation without magnetic interaction (i.e., a fully linear system), (ii) the same system with magnetic interaction, and (iii) the magnetically coupled system with a modified design parameter, namely the substrate length. In the latter case, by increasing the titanium layer length to 66 mm, the fundamental frequency decreases to 69.01 Hz (5.5% reduction), which enables the onset of bursting dynamics [4]. In this regime, a slow–fast response emerges, where the low-frequency motion at the excitation frequency coexists with a higher-frequency oscillation of the harvester, yielding higher output voltages. Fig. 2 shows the time history of the displacement for a frequency of 1 Hz, an acceleration amplitude of 2 g, and a 50 k Ω resistor. The red curve corresponds to the linear system (without magnets), the blue curve represents the enhanced response due to the selected magnetic

interaction, and the black curve depicts the bursting dynamics, in which the assigned low-frequency response is superimposed with the high-frequency response of the harvester (69.07 Hz).

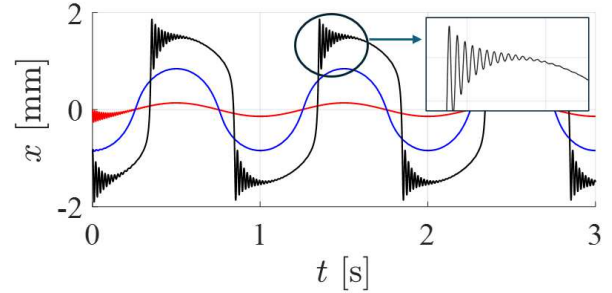


Figure 2: Displacement time history of the vibration energy harvester for excitation frequency of 1 Hz. Red: linear case, Blue: classical interwell oscillation, Black: system tuned on the bursting dynamics.

Figure 3 reports the displacement response for 7 Hz of excitation frequency. Also in this case, higher-frequency oscillations coexist with the slow response, although the regime differs: the relatively high forcing frequency prevents the complete decay of the bursting cycle.

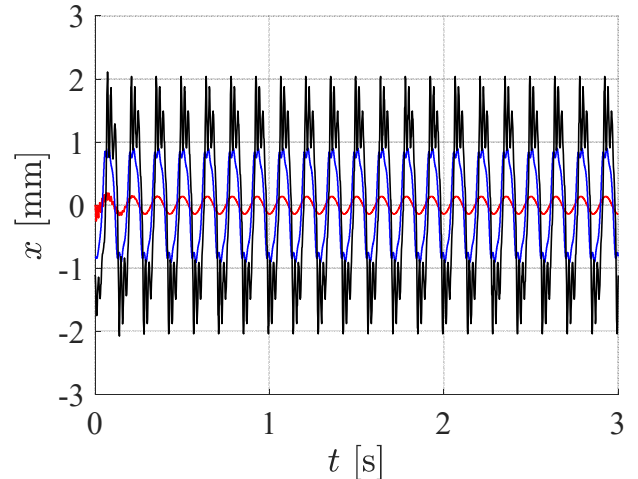


Figure 3: Displacement time history of the vibration energy harvester for excitation frequency of 7 Hz. Red: linear case, Blue: classical interwell oscillation, Black: system tuned on the bursting dynamics.

In general, bursting dynamics can be triggered by small variations in system parameters [5]. Here, the substrate length is chosen as the tuning parameter, allowing fair comparisons while keeping the PZT material, amount, and placement constant. Figures 4–6 show the phase portraits of the system voltage at 1, 3, and 7 Hz excitation. In all cases, the properly tuned system (black) exhibits enhanced instantaneous voltages compared with both the linear case (red) and the standard bistable response without bursting (blue). The yellow dots indicate the static stable equilibria of the nonlinear bistable system.

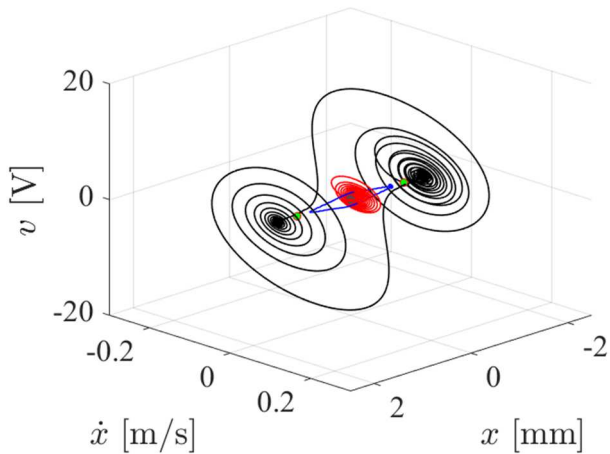


Figure 4: Phase portrait of the vibration energy harvester. Red: linear case, Blue: classical interwell oscillation, Black: system tuned on the bursting dynamics (1 Hz).

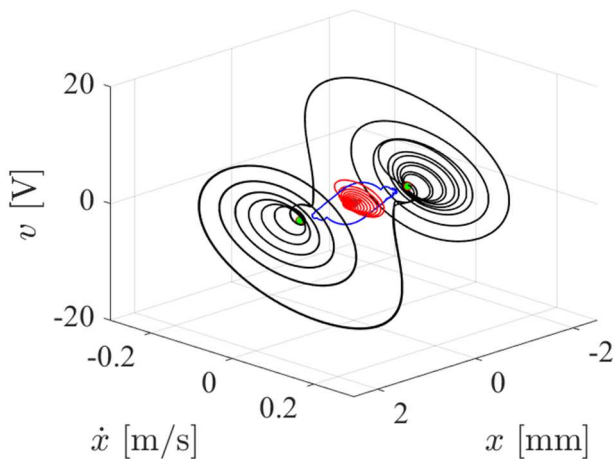


Figure 5: Phase portrait of the vibration energy harvester. Red: linear case, Blue: classical interwell oscillation, Black: system tuned on the bursting dynamics (3 Hz).

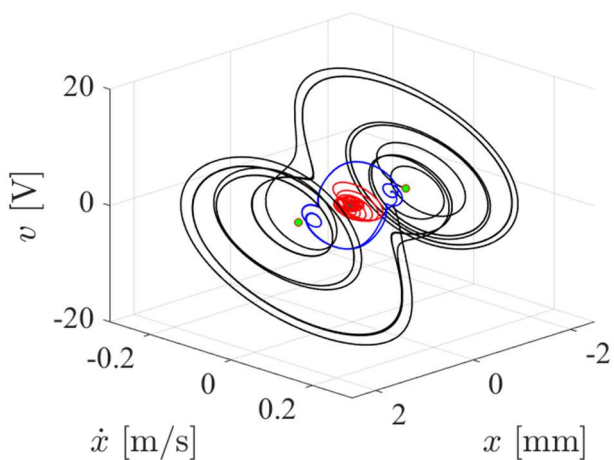


Figure 6: Phase portrait of the vibration energy harvester. Red: linear case, Blue: classical interwell oscillation, Black: system tuned on the bursting dynamics (7 Hz).

From Figures 4–6 it is evident that bursting can occur across the entire frequency range analyzed, although its persistence decreases at higher forcing frequencies. This is expected, since higher-frequency excitation does not allow the full dissipation of the high-frequency component, which typically develops around a stable equilibrium. This makes the phenomenon especially relevant for low-frequency contexts, such as human motion (< 10 Hz). An additional advantage of this regime is the realization of a frequency up-conversion mechanism in a compact configuration, without requiring additional moving masses. For completeness, Figure 7 reports the average electrical power obtained with a $50 \text{ k}\Omega$ load at 7 Hz forcing. In the bursting case, the system reaches about 3.5 mW of peak at steady state.

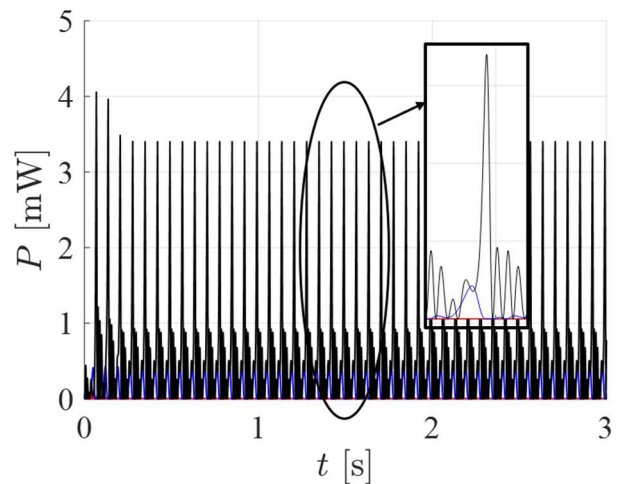


Figure 7: Instantaneous power of the vibration energy harvester. Red: linear case, Blue: classical interwell oscillation, Black: system tuned on the bursting dynamics (7 Hz).

Another relevant aspect is damping sensitivity. Figure 8 shows the response at 7 Hz with a quality factor of $Q = 20$, ten times smaller than in the previous case. Despite the increased damping, higher-frequency oscillations remain, confirming the robustness of the strategy. This makes the approach not only more effective for the analyzed device, but also attractive for practical implementations. The bursting dynamics highlighted is particularly relevant for two main reasons. First, it demonstrates that compact frequency up-conversion can be achieved without auxiliary moving masses or additional subsystems, whose design would increase complexity and overall device size. Second, the slow-fast mechanism enables efficient operation at low frequencies (down to 1 Hz), since the slow frequency forcing allows significant inter-well oscillations.

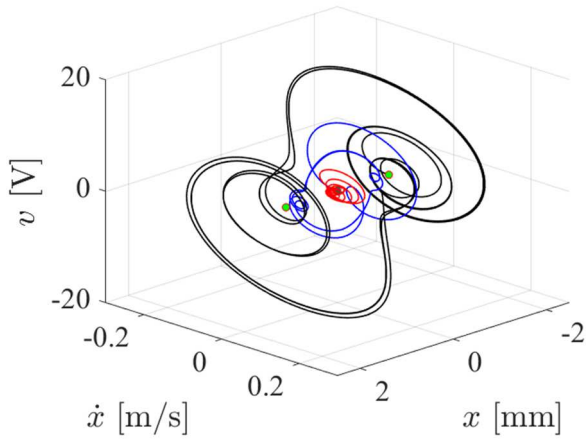


Figure 8: Phase portrait of the vibration energy harvester. Red: linear case, Blue: classical interwell oscillation, Black: system tuned on the bursting dynamics (7 Hz, $Q=20$).

CONCLUSIONS

In this work, we introduced bursting dynamics as a novel mechanism to enhance the performance of nonlinear vibration-based energy harvesters. Unlike most existing approaches that rely on additional mechanical components, such as moving proof masses or plucking mechanisms, we showed that frequency up-conversion can be achieved in a compact configuration by simply tuning structural parameters. This strategy shows that even well-established bistable layouts can exhibit previously unexplored dynamic regimes that significantly improve efficiency. The results highlight the broader potential of deliberately steering systems toward bursting regimes, opening new perspectives for the design of programmable devices that exploit nonlinearities for both vibration energy harvesting and vibration control applications. Future work will address experimental validation of the concept and the possible extension of this strategy to MEMS-scale devices.

ACKNOWLEDGEMENTS

The authors acknowledge the support of the H2020 FET-proactive project MetaVEH under Grant Agreement No. 952039.

MR wishes to thank Prof. Stefano Lenci for sharing with him some papers on bursting after MR's PhD defense.

REFERENCES

- [1] F. Cottone, H. Vocca, L. Gammaitoni, "Nonlinear energy harvesting", *Phys. Rev. Lett.*, 102, 080601, 2009.
- [2] T. Silva, D. Tan, C. De Marqui, A. Erturk, "Vibration attenuation in a nonlinear flexible structure via nonlinear switching circuits and energy harvesting implications", *Journal of Intelligent Material Systems and Structures*, 30(7):965–976, 2019.
- [3] S. Roundy, P.K. Wright, J. Rabaey, "A study of low level vibrations as a power source for wireless sensor

- nodes", *Comput. Commun.*, vol. 26, 11, 2003.
- [4] M. Rosso, E. Kohtanen, A. Corigliano, R. Ardito, A. Erturk, Nonlinear phenomena in magnetic plucking of piezoelectric vibration energy harvesters, *Sensors and Actuators A: Physical*, 362, 114667, 2023.
- [5] W.A. Jiang, X.J. Han, L. Q. Chen, Q.S. Bi, Bursting vibration-based energy harvesting, *Nonlinear Dyn.*, 100:3043–3060, 2020.
- [6] X. Han, J. Songa, Y. Zoub, Q.S. Bi, Small perturbation of excitation frequency leads to complex fast–slow dynamics, *Chaos, Solitons and Fractals*, 163, 112516, 2022.
- [7] E. M. Izhikevich, Neural excitability, spiking and bursting, *International Journal of Bifurcation and Chaos*, Vol. 10, No. 6 1171-1266, 2000.
- [8] M. Rosso, A. Corigliano, R. Ardito, "Numerical and experimental evaluation of the magnetic interaction for frequency up-conversion in piezoelectric vibration energy harvesters", *Meccanica*, 57 (5), 1139-1154 2022.

CONTACT

*M. Rosso, tel: +0223994378;
michele.rosso@polimi.it